eXPRESS Polymer Letters Vol.15, No.10 (2021) 912–928
Available online at www.expresspolymlett.com
https://doi.org/10.3144/expresspolymlett.2021.74

Morphology development to achieve electrical conductive blends based on polylactic acid/polyolefin elastomer/graphene nanoplates

Z. Saki[1], *H. Azizi*[1*], *I. Ghasemi*[1], *A. Alavi*[2]

[1]Iran Polymer and Petrochemical Institute, P.O.Box.14965-115, Tehran, Iran
[2]Department of Chemistry, University of Isfahan, 81746-73441 Isfahan, Iran

Received 6 March 2021; accepted in revised form 22 May 2021

Abstract. In the current research, to develop the morphology and improvement of electrical conductivity at low levels of graphene nanoplates (GNPs); the effect of polyolefin elastomer (POE) and graphene content on morphology, mechanical and electrical properties of polylactic acid (PLA) was investigated. Different Blends with and without compatibilizer were prepared via melt mixing process in an internal mixer through masterbatch approach. Co-continuous morphology was obtained at the ratio of 60/40 (wt%/wt%) of PLA/POE. By considering the wetting coefficient, it was predicted that graphene nanoplates have more affinity to the POE phase than PLA, which was confirmed by microscopic observations. The electrical percolation threshold was seen at 0.5–1 wt% of graphene, while the rheological percolation threshold was obtained at 0.2–0.5 wt%. The addition of POE and graphene to PLA led to balancing elongation at break and tensile strength of final products.

Keywords: *nanocomposites, polylactic acid,rheology, electrical conductivity, graphene nanoplates*

1. Introduction

Nowadays, the use of polymers in electrical conductive components has received much attention; therefore, the use of biodegradable polymers, which are a good alternative to petroleum-based products, is an interesting topic in such applications. Polylactic acid, abbreviated as PLA, is the most widely used biodegradable polymer among the biodegradable polymers because of the ease of access to lactic acid monomer and the possibility of its production on a large scale [1]. In general, PLA has good physical, mechanical and optical properties. For example, the amount of CO_2, H_2O, O_2, and N_2 transmission of PLA is less than polystyrene and more than polyethylene terephthalate. In terms of mechanical properties, PLA is brittle but has adequate strength and hardness. The tensile and flexural strength of this polymer is higher than high-density polyethylene (HDPE), polypropylene and polystyrene, but the impact strength and elongation at break are lower than the mentioned polymers. The melt viscosity of PLA, like other aliphatic polyesters, has low strength [2, 3]. In order for PLA to be used in a wide range of products, it needs physical and chemical modifications, as PLA has low melt elasticity and melt strength, as well as is brittle [4]. Alloying of different polymers is one of the most widely used methods and a common strategy to modify or improve the properties of polymeric materials [5]. There is always a need for reasonably priced elastomeric materials with good processability while maintaining their strength and elastic properties. Polyolefin elastomer (POE) has low density, high chemical, and weathering resistance. The presence of this copolymer in the blend leads to an extraordinary increase in impact resistance and therefore has been widely used in industry in recent years [6].

*Corresponding author, e-mail: H.azizi@ippi.ac.ir

Another important aspect of polymer blends is the addition of fillers to reduce the total cost or to utilize the functional properties of the material. Nanocomposites belong to this category and these properties can be given to the final materials by adding nanoparticles with special properties to one or more polymers [7, 8]. Nanocomposites can be manufactured using a solvent or melt mixing technology. For multiphase immiscible polymer blends, the addition of nanoparticles can lead to a significant increase in electrical and thermal properties [9–11]. Conductive polymer composites have an ample amplitude of applications in sensors, photovoltaic cells, electrochemical capacitors, optical devices, diodes, and electromagnetic absorbers [12–14]. Electrical and thermal conductivity can be achieved with a wide range of conductive nanoparticles such as Ag, Au, Pd, Pt, carbon nanotubes (CNTs), and graphene (GNPs) [15, 16]. GNP with a Young modulus of 1 TPa and final strength of 130 GPa is known as the most resistant material. The thermal conductivity of GNP is 5000 W/(m·K), which is equivalent to the highest thermal conductivity reported for CNTs. Besides, the high electrical conductivity of 6000 S/cm and the surface area of 2630 m^2/g are the characteristics of this material [17–19] which indicate GNPs' high thermal, mechanical, electrical, and gas impermeability properties. Ethylene-octene copolymer is a POE used by Hou *et al*. [20] for blending with PLA by using POE-*g*-PLA copolymer as a compatibilizer. In 2019, Huang *et al*. [21] published a review article about the invention of multi-component and multiphase electrically and thermally conductive composites which revealed that specific placement of various fillers in different co-continuous phases can result in several functionalities, including high electrical and thermal conductivity, also electromagnetic interference shielding. More prepossessingly, Marischal *et al* [22] prepared three types of two-component polymer composites with polycaprolactone (PCL) fixed component and variable polymers of PP, PA6, and PET, added the MWCNT filler, and reported different properties of prepared samples. Hadaeghnia *et al*. [23] claimed PA6/ POE blend with an unstable co-continuous morphology which the addition of GNPs led to a stable co-continuous morphology for composition near to phase inversion. Recently, Luo *et al*. [24] reported the preparation of polylactic acid/ high-density polyethylene/carbon black (PLA/HDPE/CB) composites by a two-step method and studied double percolation threshold. In the case of rheological investigation of blends, in 2017, Wang *et al*. [25] investigated the rheological properties of (poly(vinylidene fluoride)/poly(L-lactide)) blends (PVDF/PLLA/nSi) which by localization of jammed Janus Grafted Silica (JGS) at the interface of this polymer blend the nano-network formation was improved. Also, in 2018, Zhao *et al*. [26] incorporated the CNTs with active epoxy and PMMa-tails groups into PVDF/PLLA immiscible blend. The results of electrical conductivity showed that the pure blend without CNTs had about 6 orders less conductivity than the blend containing functionalized CNTs.

This study aimed to develop the morphology and achieve a grafted structure that improves the electrical conductivity of nanocomposites constructed by PLA and POE blend in the presence of GNPs at low wt% content of filler. This blending was performed to better dispersion of GNPs in a two-step process through melt mixing.

2. Experimental

2.1. Materials

Polylactic acid (PLA) grade of 2003D, was a commercial product of NatureWorks Co., polyolefin elastomer (POE) with a grade of Vistamaxx™6202 was purchased from ExxonMobil Co. (composed of randomly distributed isotactic propylene repeating unit with ethylene). The graphene nanoparticles (GNP) that were provided by Angstrom were in the grade of N002-PDR.

2.2. Methods

To achieve a co-continuous morphology and study the trend of morphological changes from matrix-droplet to the co-continuous morphology, PLA and POE were blended in different ratios. For this purpose, PLA was placed in an oven at 70 °C for 12 hr. The polymers were then mixed using a Brabender type internal mixer for 7 min at 180 °C and rotation speed of 60 rpm; then samples were prepared with different proportions. To predict the optimum composition resulting in co-continuous morphology, several experimental and quasi-experimental models in terms of material properties and process conditions have been developed over the past three decades. For this object, Equation (1) was used, which Paul *et al*. [27] proposed using the viscosity ratio of mixed components. Also, Miles and Zurek [28] developed the proposed equation using dynamic viscosity under

mixing conditions for alloys with high differences in viscosity values. Therefore, in this study, to calculate the co-continuous composition, Equation (1) was utilized in which the shear viscosities of PLA and POE were measured from their dynamic viscosities:

$$\frac{\varphi_1}{\varphi_2} = \frac{\eta(\gamma)_1}{\eta(\gamma)_2} \quad (1)$$

where φ_1 and η_1 are POE weight fraction and viscosity, also φ_2 and η_2 are weight fraction and viscosity of PLA, respectively, γ is constant shear rate.

After the co-continuity acquisition for the PLA/POE blend, to add nanoparticles to the blend, considering better dispersion of the material in the diluted masterbatch, first, a masterbatch of polyolefin elastomer with 4 wt% GNP were prepared and then mixed in a molten state with PLA. The total required masterbatch was prepared in one process with Brabander internal mixer at 150 °C and rotation rate of 60 rpm for 10 min. Then was diluted with PLA in different weight ratios of graphene so that the weight ratio of PLA and polyolefin elastomer was 60 to 40. The dilution process was performed at 180 °C, at the rotation speed of 60 rpm for 7 min. Afterward, the samples were molded at 200 °C for 4 min at 35 MPa pressure with Toyoseiki hot press apparatus. Table 1 shows the formulation and coding of the prepared samples.

2.3. Contact angle analysis

To determine the surface tension of PLA and POE, the contact angle measurement was carried out using the sessile drop method in the air atmosphere. The experiments were performed at room temperature, and the surface tension of these samples was specified by dripping drops of two liquids, water and diiodomethane. For each sample, at least 4 drops of each liquid were dropped on the surface, and the average contact angle was reported. The device applied contact angle test was Kruss G10 made in Germany. To measure the surface tension of polymers, sheets with a thickness of 1 mm were prepared using a hot press device. It is noteworthy that measuring the surface tension of graphene nanoplates was not possible with the mentioned method. This was due to the adhesion of graphene nanoparticles to a metal cylinder, which was used for compression to make tablets.

Table 1. The formulation and coding of the prepared samples.

Sample	Weight ratios of (PLA/POE)
PLA90/POE10	90/10
PLA80/POE20	80/20
PLA70/POE30	70/30
PLA60/POE40	60/40
PLA50/POE50	50/50
PLA40/POE60	10/60
PLA60/POE40 blend was selected as optimum and nanoparticles were added.	
PLA60/POE40/GNP0.2	Containing 0.2 wt% GNP
PLA60/POE40/GNP0.5	Containing 0.5 wt% GNP
PLA60/POE40/GNP1	Containing 1.0 wt% GNP
PLA60/POE40/GNP1.5	Containing 1.5 wt% GNP

2.4. Determination of the filler surface tension

To evaluate the surface energy of the filler, the capillary rise method was performed. Water and diiodomethane were used as solvents. Then, having the surface tension of the solvent and the contact angle of the nanoparticle-solvent, the polar and distributive parts of the surface tension of graphene nanoplates were determined. In this method, the desired powder is exposed to the solvent, and the weight of the solvent absorbed by the sample is determined over time. Then, using Equation (2), the contact angle for each of the solvents used is obtained [29, 30]:

$$W^2 = C\frac{\rho^2 \gamma_L \cos\theta}{\eta} \quad (2)$$

where W is the added weight, ρ, γ_L and η are the density, surface tension, and viscosity of the fluid, respectively. C represents a geometric factor that is related to the packing density and material size. To specify the geometric factor, normal heptane is considered as the reference fluid, and the contact angle between the powder and normal heptane is taken to be zero. Using the contact angles obtained for the two solvents, the polar and dispersive parts of the powder surface tension can be obtained according to the Fox equation (Equation (3)) [31].

$$\frac{1}{2}\frac{\sigma_l(1+\cos\theta)}{\sqrt{\sigma_l^d}} = \frac{\sqrt{\sigma_s^p \sigma_l^p}}{\sqrt{\sigma_l^d}} + \sqrt{\sigma_s^d} \quad (3)$$

where σ_s^p and σ_s^d are the polar and dispersive components of the surface tension of the solid substance and σ_l^p and σ_l^d are the definite components of the surface tension (polar and non-polar) of the fluid and the wetting angle of the solvent-solid powder.

2.5. Scanning electron microscopy (SEM)

Information about the morphology of the phases was assessed by SEM analysis. Imaging of the fractured surface of the samples was performed without etching. A Scanning Electron Microscope made by the TESCAN company of the Czech country was utilized to characterize the prepared samples.

2.6. Energy dispersive X-ray analysis (EDX)

As either component extraction of the surface was not possible, the EDX test was used to detect each phase. In this test, the INXA model EDX analyzer made by Oxford Instrument Co. was taken advantage.

2.7. Electrical conductivity analysis

For conductivities lower than 10^{-6} S/cm, the electrical properties of the samples were measured by Solid-State Electrometer 610C Equipment Keithley Instruments, and for conductivity values higher than 10^{-6} S/cm, the multimeter device of BK Precision Bench Digital Multimeter Model 5491A made in the USA was used.

2.8. Rheological measurement

The storage modulus (G') and complex viscosity (η^*) of specimens in terms of angular frequency (ω) were measured in frequency sweep using an oscillatory rheometer (Physicaanton Paar-MCR-30, Germany) with a 25 mm parallel plate in diameter and a gap of 1 mm. The test was implemented in the range of 0.01–600 S^{-1} frequency and pre-heating time of 2 min. The tests were conducted under a nitrogen atmosphere to prevent oxidation of the sample. This test was carried out at a temperature of 180 °C and in the frequency range of 0.01–600 rad/s. Also, to set the samples in the linear viscoelastic region (LVE), a 1% strain was selected for the frequency scanning test.

2.9. Mechanical properties

In order to study the mechanical properties of pure PLA, POE, and blend of PLA/POE/GNPs, the tensile test was applied to the samples. In this study, a Santam STM-20 device made in Iran equipped with a film jaw was utilized. Samples were prepared as dumbbells with a thickness of 1 mm and a distance between two jaws of 25 mm according to ASTM D638-5. The test speed was adjusted to 50 mm/min.

3. Results and discussion

3.1. Predicting the location of GNP

It is perspicuous that to specify the location of graphene nanoparticles is essential in determining the final morphology and controlling the properties of the immiscible blend. In general, the location of filler in an immiscible mixture strongly depends on the surface properties of the components. The selective placement of GNP in one of the two phases is due to its tendency towards these two phases. The surface tension of all present components, including the two polymer parts and GNP, was calculated by measuring their contact angle. Obviously, contact angle measurements are affected by many factors such as surface roughness, material composition, surface crystallinity, and so on.

There are different theories to calculate the interfacial tension of two phases. According to Wendt, Owens, Kealble, and Rabel methods, interfacial tension can be calculated by Equation (4):

$$\gamma_{ij} = \gamma_i + \gamma_j - 2\left(\sqrt{\gamma_i^d \gamma_j^d} + \sqrt{\gamma_i^p \gamma_j^p}\right) \tag{4}$$

This equation, known as the geometric mean, is more suitable for polar systems. Another equation proposed by Wu is called the harmonic mean (Equation (5)):

$$\gamma_{ij} = \gamma_i + \gamma_j - 4\left(\frac{\gamma_i^d \gamma_j^d}{\gamma_i^d + \gamma_j^d} + \frac{\gamma_i^p \gamma_j^p}{\gamma_i^p + \gamma_j^p}\right) \tag{5}$$

This model is more favorable for lower energy systems such as organic solutions, polymers, and organic pigments. To indicate the location of filler particles within the phases of a polymer blend, the wetting coefficient (ω), defined by Equation (6) is a suitable method:

$$\omega = \frac{\gamma_{bc} - \gamma_{ac}}{\gamma_{ab}} \tag{6}$$

where γ is the interfacial energy of components, *a* and *b* represent two polymers, and *c* denotes the filler. The value of ω determines the equilibrium state of nanoparticles. If ω is more than 1, the nanoparticle will be in phase a, if it is less than –1, it will be in phase b, and if it is between 1 and –1, the nanoparticle will be in the junction of the two phases [32]. The results related to the surface tension of the samples are presented in Table 2.

Table 2. The surface tension of polymers and GNP.

Material	Total surface tension [mN/m]	Distributive component of solid part (σ_s^d) [mN/m]	Polar component of solid part (σ_s^p) [mN/m]
GNP	50.80	0.1652	50.9652
PLA	30.51	9.8400	40.3500
POE	31.70	0.1900	31.8900

Table 3. Interfacial tensions and wetting coefficients based on mean geometric and harmonic equations.

Materials	Interfacial tension (γ_{ij}) [mN/m]		Wetting coefficient (ω)		GNP location
	mean geometric equation	harmonic equation	mean geometric equation	harmonic equation	
PLA, POE, GNP	γ_{ab} = 1.011	γ_{ab} = 8.961	1.061071	1.066487	POE
	γ_{ac} = 2.296	γ_{ac} = 4.528			
	γ_{bc} = 2.735	γ_{bc} = 14.084			

POE, PLA, and GNPs are considered as components *a*, *b* and *c*, respectively. According to the illustrated results in Table 3, the value of ω for GNPs, based on both mean geometric and harmonic equations, was greater than 1. Therefore, it was indicated the presence of nanoparticles in polymer a, (POE). It is important to note that in previous studies, there was no common agreement on data on the surface energy of polymers, even using similar methods such as contact angle measurements. For example, in a study on PLA for polar component, distributive component, and total surface energy, the researchers reported values of 10.5, 29.7, and 40.2 mJ/m^2, respectively, and in another study, the values of 3.9, 39.6, and 43.5 mJ/m^2, were obtained, which indicated that the surface energy of PLA varies from 35.9 to 45.9 mJ/m^2 depending on the sample preparation [33, 34].

3.2. Morphology of PLA/POE blends

The physical and mechanical properties of blends depend on the thermodynamics of their mixing. The properties of miscible and semi-miscible blends depend not only on the properties of each phase but also on the morphology and adhesion between the phases [35]. SEM technique was performed to investigate the distributed phase morphology in the blend. Therefore, according to the results obtained by the extraction method, the SEM image was taken from the cross-section of the samples without extracting any of the phases. Figure 1 showed the cross-section of the samples containing different amounts of POE without extraction. In blends with low contents of the POE phase matrix-droplet morphology was observed. As demonstrated in Figure 1, with increasing the POE content, the size of the droplet phase increases, which indicates the occurrence of the coagulation phenomenon. According to Equation (1) and the setting of both phases' viscosity, the combined phase inversion percentage (co-continuity) was calculated to be 40 wt% of POE. Therefore, increasing the amount of POE to about 40 wt% is expected to lead to the formation of a co-continuous morphology. Figure 3d showed that both phases had preserved their continuity. Also, at higher amounts of POE, the blend underwent phase inversion, and the matrix-droplet morphology reappeared, which POE composed the matrix phase (Figures 3e and 3f). The phase change was also confirmed by EDX analysis.

3.3. The effect of GNPs on the co-continuous morphology of PLA/POE blend

The purpose of adding GNPs is to increase the electrical conductivity of the samples. Studies showed that the use of co-continuous morphology and the achievement of double bonding leads to the electrical conductivity of the samples in lower amounts and better distribution of nanoparticles throughout the sample. Different contents of GNPs were added to the PLA60/POE40 blend, and the morphological alterations were evaluated. Figure 2 showed the cross-section morphology of blends containing different amounts of GNPs. Figure 2a is the reference sample without nanoparticles, and as can be seen, each of the phases is relatively in size large and evident. Figures 3b to 3e are samples containing different amounts of GNPs. As the nano content was increased, the size of the phases became smaller and finer, so that the samples still retained their co-continuous structure.

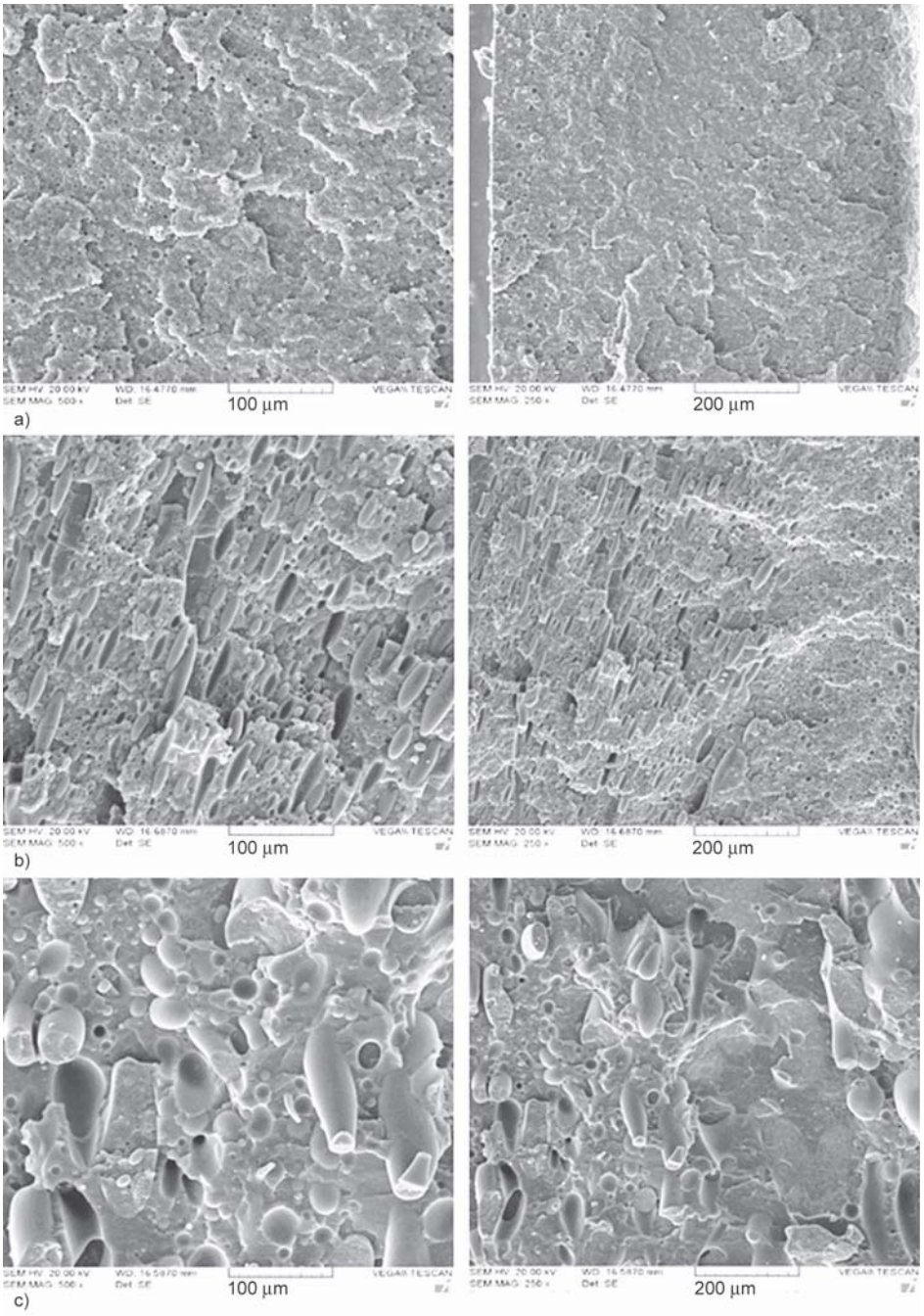

Figure 1. The cross-section of the samples containing different amounts of POE: (a) PLA90/POE10, (b) PLA80/POE20, (c) PLA70/POE30 (all images were reported at scales of 100 and 200 µm).

Bose *et al*. [36], in a study of PA6/ABS co-continuous blends morphology, claimed that with increasing the quantity of MWCNT, the co-continuous structure was shrunken. Nonetheless, the co-continuous structure in the series of blends was observed by increasing the MWCNT concentration.

3.4. EDX analysis

To identify each phase the EDX test was implemented. Figure 3 depicted the EDX spectrum of two different sections in each sample. The structure of POE contains carbon and hydrogen elements, and PLA includes carbon, hydrogen, and oxygen. Since both phases had light in weight and possessed common elements, a good element distribution map was not obtained. Therefore, identification was performed only at one point of each phase, and the corresponding peak was obtained. In Figure 3a, only the peak of the carbon in the phase with a smooth surface was observable, which was an indicator of the POE surface character. Also, the oxygen and carbon peaks in the phase with a rough surface indicating the PLA

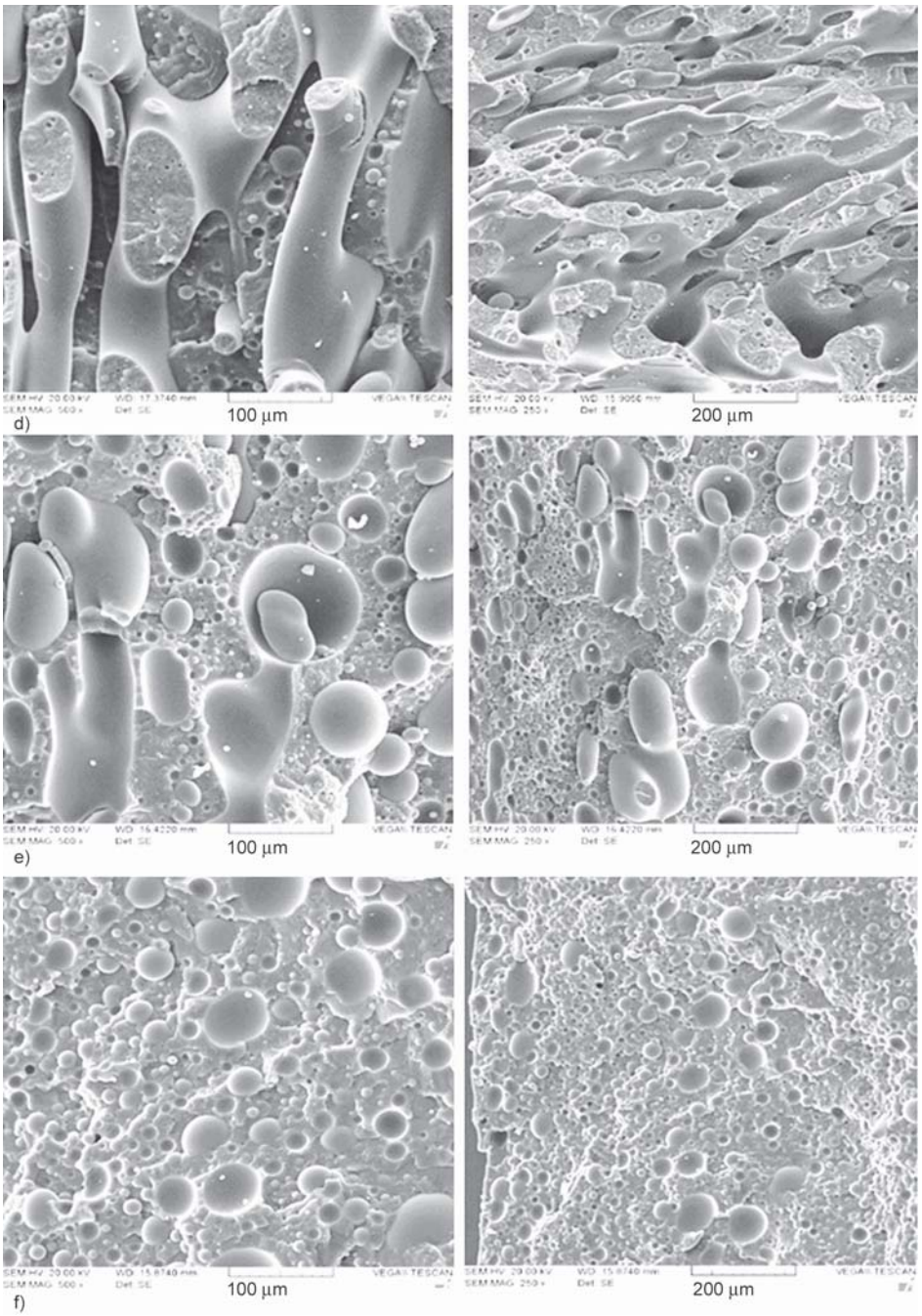

Figure 1. The cross-section of the samples containing different amounts of POE (continuous): (d) PLA60/POE40, (e) PLA50/POE50, (f) PLA40/POE60 (all images were reported at scales of 100 and 200 µm).

phase (Figure 3b). In addition, in Figure 3c, 3d, the phase inversion for the 50-50% composition could be seen. Thus, POE represented the matrix phase, and PLA deputed the drop phase.

3.5. Electrical conductivity analysis

The effect of graphene nanoplates and co-continuous morphology of non-miscible PLA/POE blend on the electrical conductivity was investigated. Since in this research, PLA and POE were used, which are non-conductive, the presence of conductive fillers such as GNPs provides the electrical conductivity of these polymers. The electrical conductivity of PLA60/POE40 blend nanocomposites as a function of nanparticle content was exhibited in Figure 4. The results showed that with increasing the concentration of nanoparticles, the conductivity of the nanocomposite was mutually increased. The maximum conductivity was obtained in the sample containing 1.5 wt% of GNPs. Also, an abrupt increase in conductivity slope was observed in the range of 0.5 to 1 wt% of GNPs. The reason for the increase in these

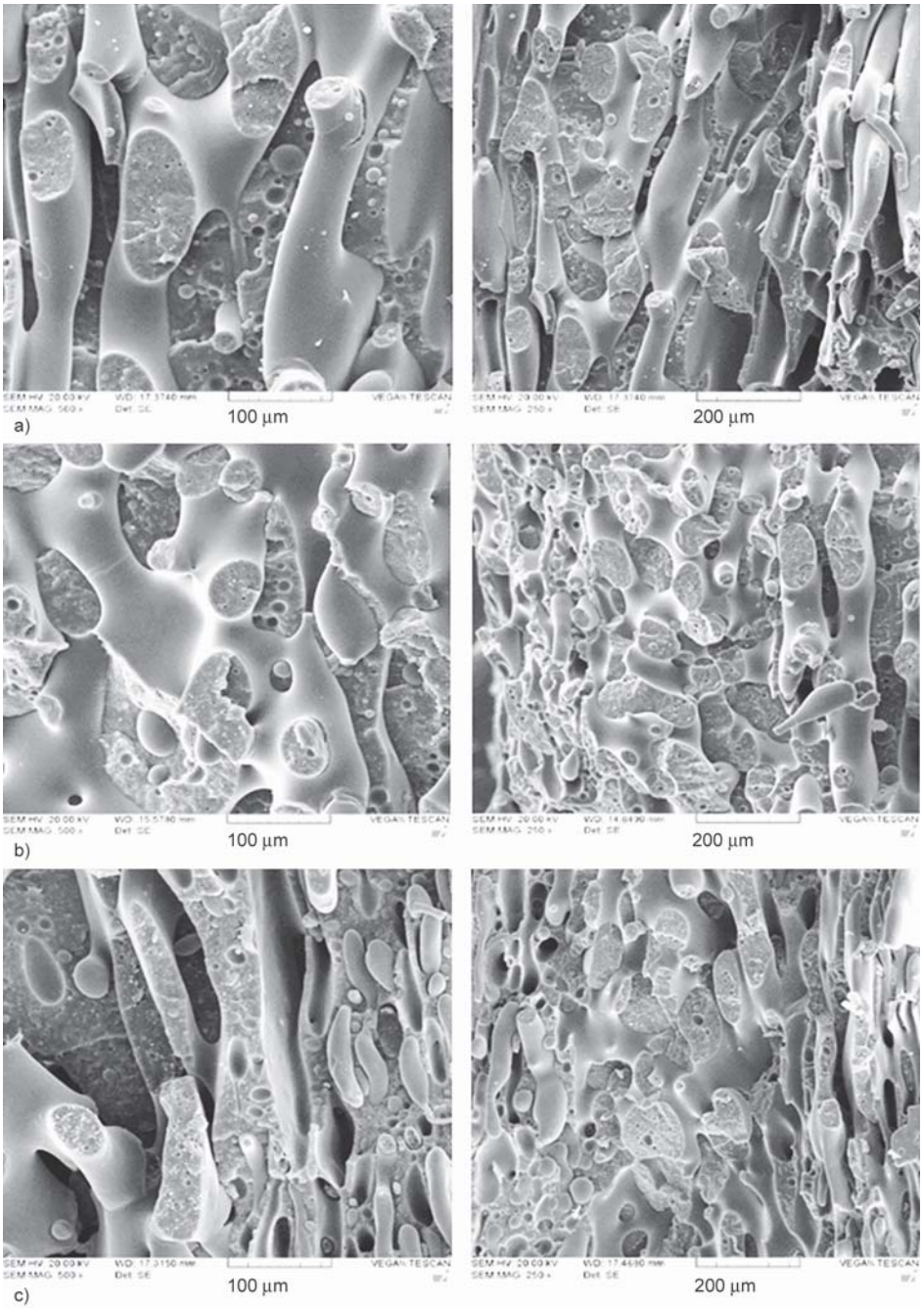

Figure 2. The cross-section morphology of blends without extraction containing different amounts of GNPs: (a) PLA60/POE40, (b) PLA60/POE40/0.2GNP, (c) PLA60/POE40/0.5GNP (all images were reported at scales of 100 and 200 µm).

concentrations can be attributed to the formation of a conductive lattice structure and continuous electronic paths in the nanoparticles, the increase in the number of contact points of conductive particles, and the arrival of the nanocomposite at the percolation threshold. The mechanism considered to explain this phenomenon is the procedure of electrical tunneling, which is assumed to allow a high volume of electrons to pass through the sample due to the formation of conductive channels at high amounts of the filler, and the conductivity increases [37, 38]. Also, the existence of a co-continuous structure has resulted in electrical conductivity at lower concentrations of nanoparticles.

3.6. Rheological properties of nanocomposites

To determine the rheological properties of the nanocomposites, a frequency scanning test was performed. Therefore, the dynamic variables of storage modulus (G'), loss modulus (G''), complex viscosity

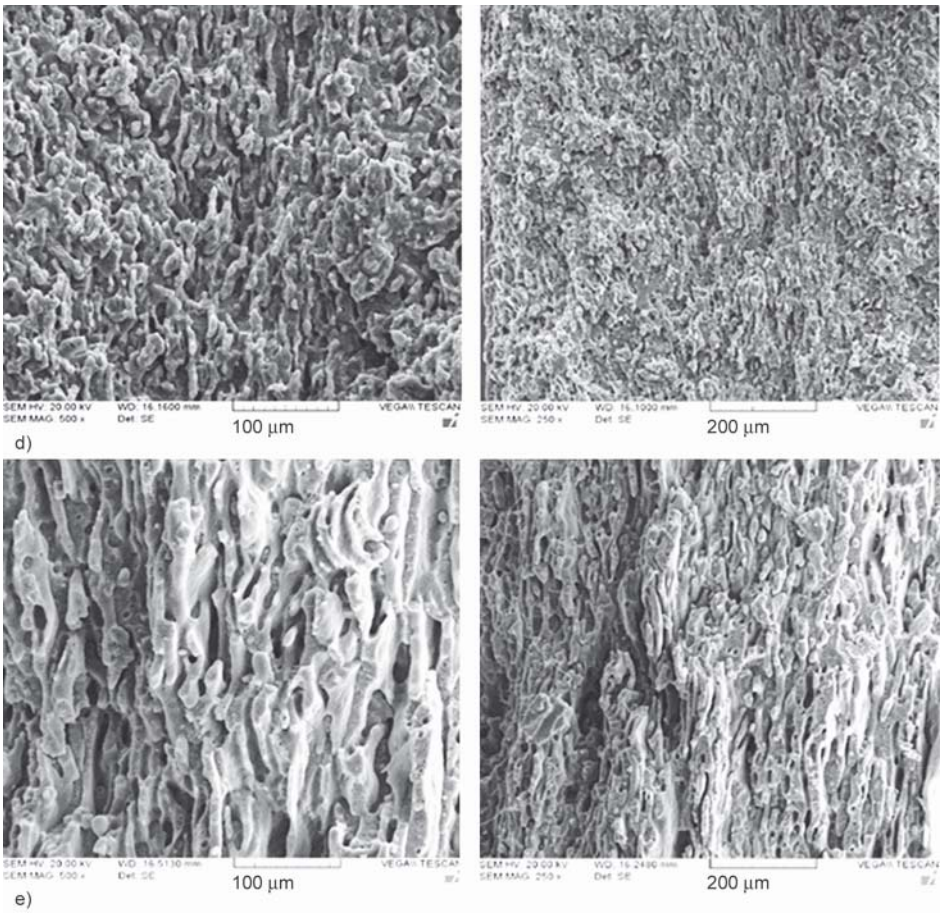

Figure 2. The cross-section morphology of blends without extraction containing different amounts of GNPs (continuous): (d) PLA60/POE40/1GNP, (e) PLA60/POE40/1.5GNP (all images were reported at scales of 100 and 200 µm).

(η^*) and loss factor ($\tan\delta$) were calculated and plotted in terms of angular frequency (ω). The G' and G'' curves of PLA, POE, PLA60/POE40 blend, and nanocomposites based on this blend containing different amounts of GNPs are illustrated in Figures 5 and 6. As shown in the figures, by the increment in the quantity of GNPs, both the storage modulus (G') and the loss modulus (G''), especially at low frequencies, are increased compared to the pure sample. At low frequencies, polymer chains are completely relaxed, and the storage module behavior (Figure 5) followed the classical linear viscoelastic diagram, also called the terminal or liquid-like behavior. As the amount of GNPs increased, this final behavior was eliminated in the low-frequency range, and a plateau is observed, which is called non-terminal or solid-like behavior, and the dependence of G' and G'' on the frequency was diminished. Therefore, the presence of GNPs significantly prevented the polymer chains' relaxation in the blend components. By increasing the values of GNPs to more than 0.5 wt%, at low frequencies, G' would almost be independent of frequency, indicating a transition from liquid-like to solid-like viscoelastic behavior. This non-terminal behavior at low frequencies and the occurrence of the flat area of G' can be related to the formation of a graphene nanoplates network that surrounds the entire sample and prevents the movement of polymer chains. As can be seen in Figure 5, the length of the flat area had a straight correlation with the concentration of GNPs, and both of them are increased together, which indicated the formation of a stronger lattice structure due to the nano-nano and nano-polymer chain interactions [39]. The same trend with a lower rate was observed for loss modulus alterations.

In the curve of Figure 7, the variations of the complex viscosity (η^*) in terms of frequency were also illustrated in the rheological response with increasing GNPs. The complex viscosity of blends increased with raising the GNPs content, and this increase was more intense at low frequencies but gradually got decreased with increasing frequency due to the shear thinning behavior. As shown in Figure 7, η^* of pure PLA and POE showed a Newtonian region at low frequencies. This behavior was also observed in PLA60/POE40 blend. When GNPs were added to

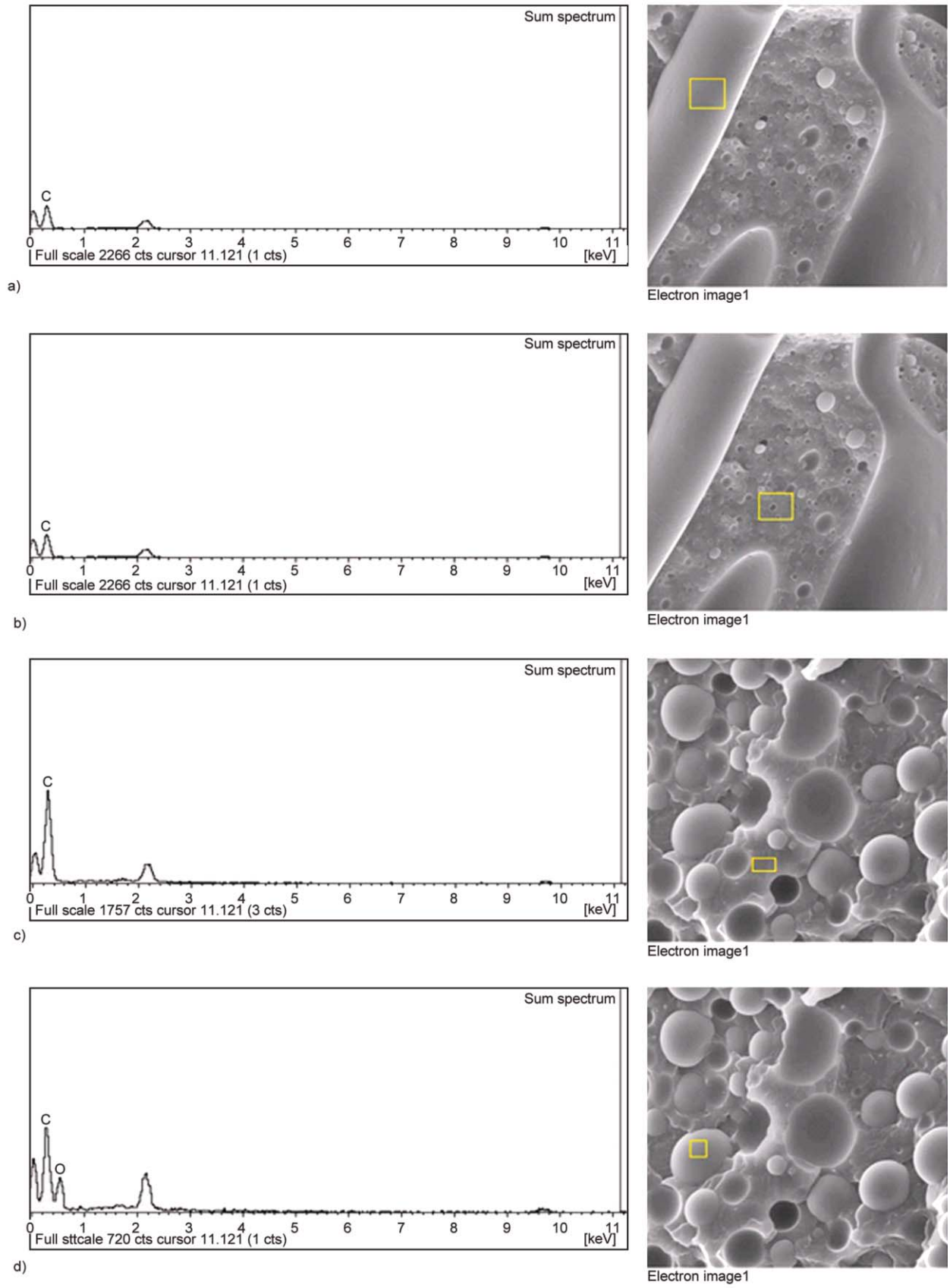

Figure 3. The EDX spectrum of two different parts in each sample of; (a, b) PLA60/POE40, (c, d) PLA50/POE50.

the blend, the behavior in the frequency range became nonlinear, and the frequency dependence increased so that the Newtonian linear region was not observed, indicating the elastic behavior of these materials,

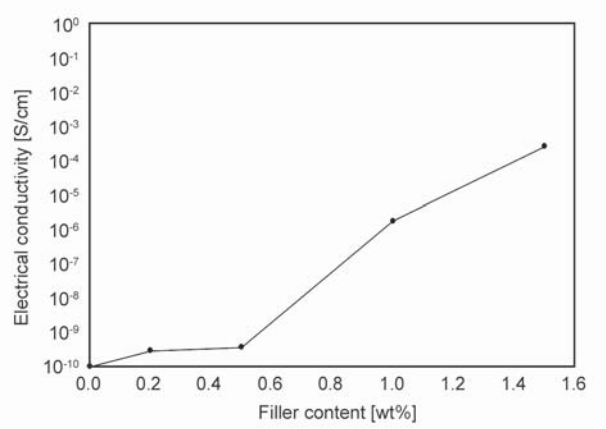

Figure 4. The electrical conductivity of PLA60/POE40 blend nanocomposites as a function of nanoparticle content.

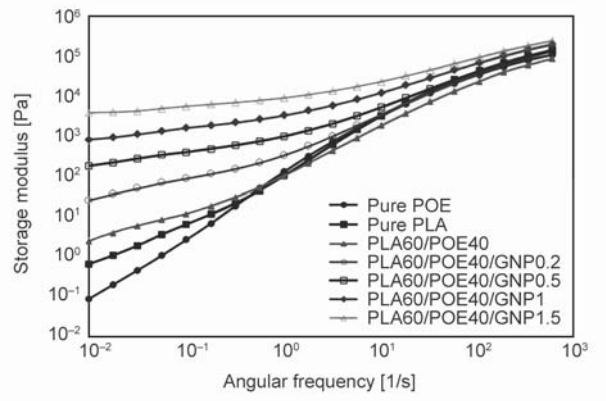

Figure 5. The storage modulus of nanocomposites based on PLA60/POE40 blend in terms of angular frequency.

which is due to the increased interactions between GNPs and polymer chains and the formation of an interconnected network of filler particles. At low angular frequencies, the polymer chains of the neat samples had enough time to relax to the equilibrium state, and thus the molten samples showed a flat area

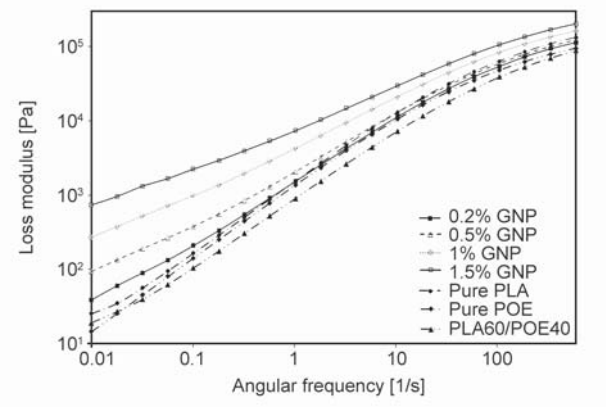

Figure 6. The loss modulus of nanocomposites based on PLA60/POE40 blend in terms of angular frequency.

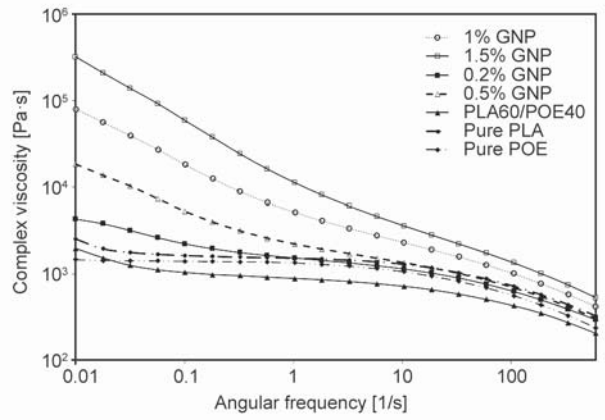

Figure 7. The complex viscosity of nanocomposites based on PLA60/POE40 blend in terms of angular frequency.

of Newtonian viscosity. After the addition of GNPs, η^* showed an increase that indicates an increase in flow resistance, which limited the relaxation of polymer chains. As the filler content increased, the interaction between the nanoparticles and the polymer propagated, resulting in the formation of an overlapping network and, ultimately, the transition from liquid-like to solid-like state. Also, because the temperature of the melted POE compared to the PLA was much lower than the test temperature, the PLA had a higher viscosity than POE.

The damping characteristics of nanocomposites based on PLA/POE blend were also studied by examining the relationship between the damping parameter ($\tan\delta$) and the angular frequency (Figure 8). It was observed that $\tan\delta$ was decreased especially at lower frequencies, by the increment in the content of nanoparticles. This behavior represented the strong interfacial interactions between GNPs and polymer chains. In fact, the increase in nanoparticle content

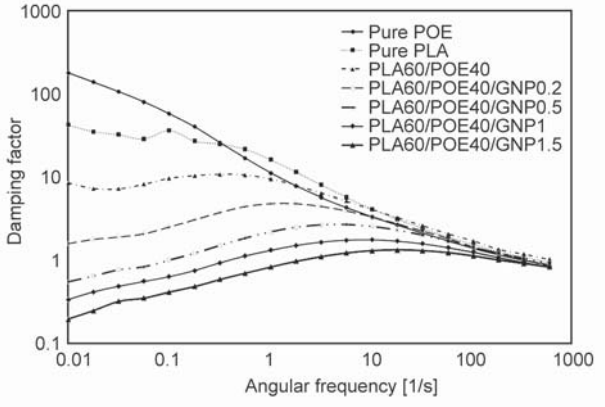

Figure 8. The damping ($\tan\delta$) of nanocomposites based on PLA60/POE40 blend in terms of angular frequency.

limited the relaxation of the chains. Also, the reduction of the loss factor for the filler-free sample compared to the pure polymers was due to the fact that by increasing the ratio of PLA to POE, stronger interactions were originated in the interface of two-phase and the loss factor was reduced, and elasticity was raised. This increase in elasticity for nano-free blends can also be seen in the storage modulus in terms of the frequency diagram.

Figure 9 portrayed the Cole-Cole diagram of pure PLA and POE, as well as nanocomposites based on the blend of two polymers. When a regular half-crescent was seen in the Cole-Cole diagram, the deformation behavior of the material could be described by the single relaxation time or the narrow distribution of relaxation time. In complex systems, the presence of several relaxation times caused some changes in the order of the crescent [40, 41]. In Figure 9, the pure PLA and POE have half crescent-like shapes, while the shape of the graph was changed with the addition of nanoparticles. In 0.2 wt% of GNPs, two regions were observed. A half-crescent region at low viscosities can be attributed to the dynamics of POE chains and a linear region at high viscosities that may be due to the graphene-graphene network or the relaxation time of POE chains as a result of interaction with GNPs. With 0.5 wt% of GNPs, the semi-crescent region became shorter, and at 1 and 1.5 wt%, this region was disappeared, and the slope of the linear region turned steeper. This behavior could be due to a reduction in the dynamic relaxation of polymer chains because of the formation of stronger polymer-filler networks, which would lead to a longer relaxation time. Navas *et al*. [32] achieved similar results for PS/PP blend in the presence of carbon nanotubes.

In the study of the rheological behavior of filled polymers, the transition in the viscoelastic behavior of the system from liquid-like ($G'' \propto \omega^1$, $G' \propto \omega^2$) to solid-like (G' and $G'' \propto \omega^0$) has always been of interest to researchers. The concentration of the filler is known as the percolation threshold to the extent that this transfer occurs. This liquid-solid transition can be characterized by the Van Gurp-Palmen curve. This curve relates the value of the phase angle (δ) to the complex modulus (G^*). The phase angle is a very sensitive rheological factor to the threshold of nanocomposite lattice formation which the liquid-like behavior of melt is described by $\lim_{G^* \to 0} \delta = 90°$ while

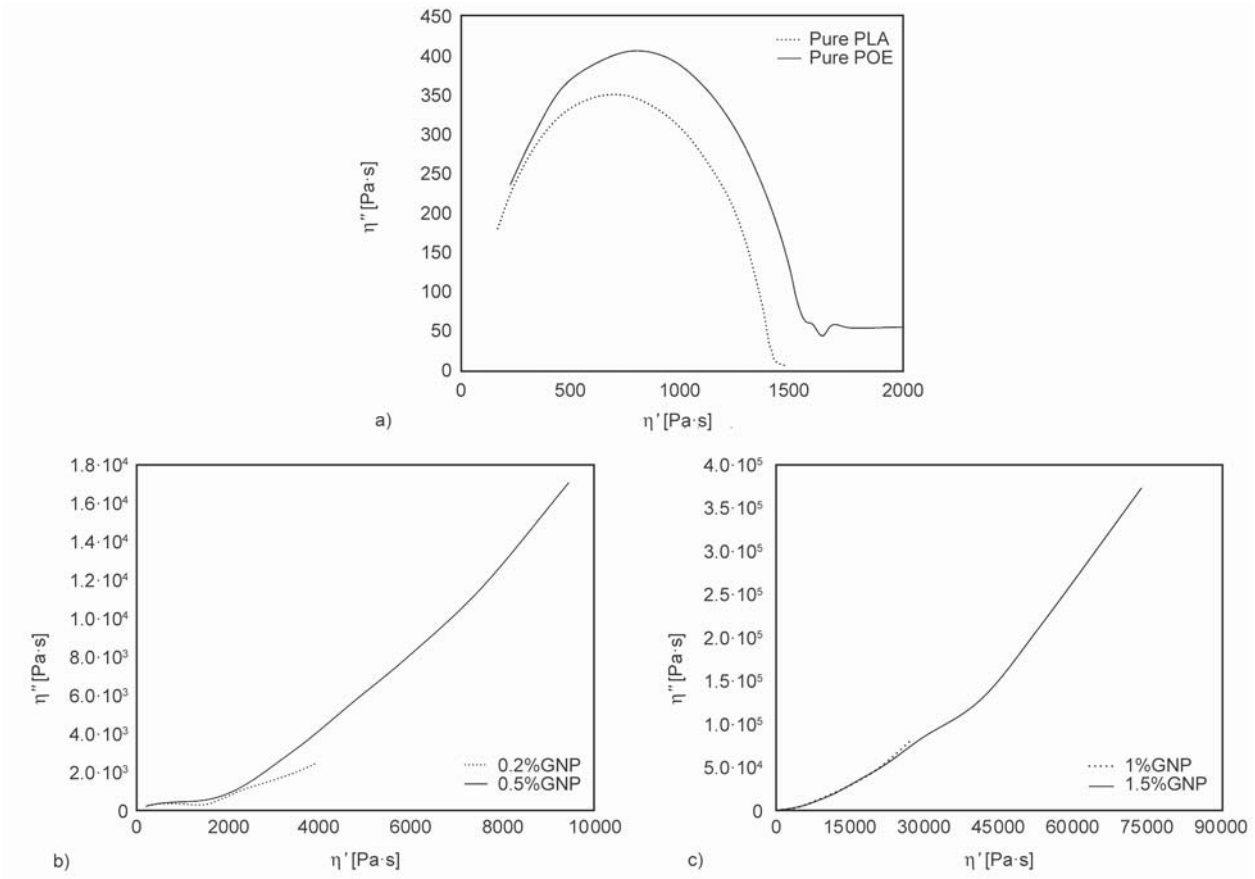

Figure 9. The Cole-Cole diagrams of (a) neat PLA and POE, (b) PLA60/POE40/GNP0.2 and PLA60/POE40/GNP0.5 blends, (c) PLA60/POE40/GNP1 and PLA60/POE40/GNP1.5 blends.

for solid-like behavior, δ significantly reduces regarding the G^* decrement [42]. The Van Gurp-Palmen curves for PLA, POE, PLA60/POE40 blend, and the corresponding nanocomposites containing different contents of GNPs are shown in Figure 10. It was observed that the value of phase angle for pure polymers is close to 90 degrees, and with the addition of GNPs, the phase angle was reduced and reached its lowest value at 1.5 wt% of GNPs. In this system, the first dominant raise of the phase angle towards the pure polymer was related to the nanocomposite containing 0.2 wt% of GNP, which indicated that the beginning of the rheological percolation threshold occurs in this region.

In order to more accurately determine the region of behavior-changing from liquid-like to solid-like state, in other words, the rheological percolation threshold of GNPs to the blend, the storage modulus at a fixed frequency was evaluated. In Figure 11, the diagram of the normalized storage modulus of PLA/POE/GNP nanocomposites in terms of GNP quantity is shown.

Different theories, including percolation theories, are used to study this phenomenon quantitatively. According to the percolation theory, the following equation (Equation (7)) can be used to calculate the rheological percolation threshold:

$$G_0' \sim (\phi - \phi_{cG'})^{\nu} \tag{7}$$

where G_0' is the storage modulus, ϕ the volume fraction of the filler, $\phi_{cG'}$ is the rheological percolation threshold, and ν is the elastic exponent attributed to the stress-bearing mechanisms [43]. Therefore, by fitting Equation (7) to the storage modulus curve in terms of weight percentage of GNPs, the exact value

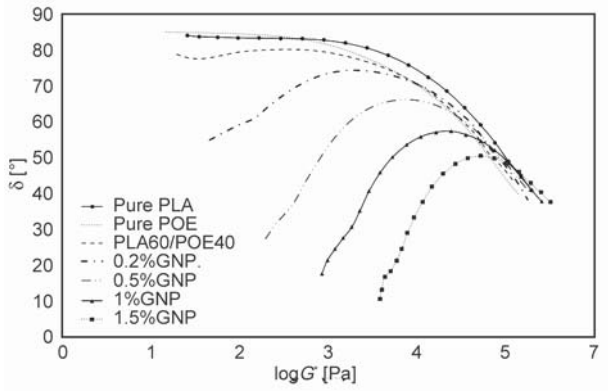

Figure 10. The Van Gurp-Palmen curves for PLA, POE, PLA60/POE40 blend, and the nanocomposites containing different contents of GNPs.

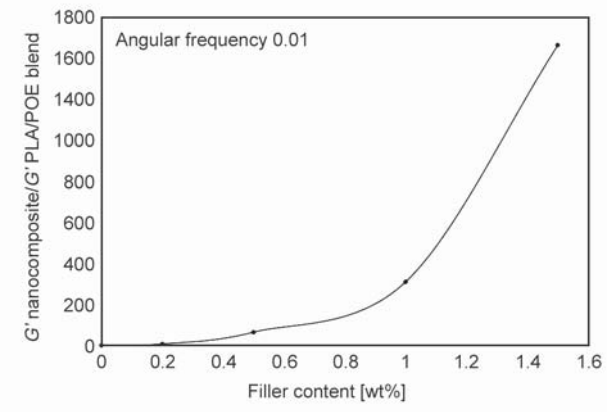

Figure 11. The diagram of the normalized storage modulus of PLA/POE/GNP nanocomposites in terms of GNP content.

of rheological percolation of 0.437 wt% of GNPs was obtained. Therefore, the range in which the rheological percolation threshold occurred was between 0.5–2 wt% of GNPs. The obtained value confirmed the rheological percolation threshold acquired by the Van Gurp-Palmen curve.

On the other hand, to take place the electrical percolation, GNPs must be in close juxtaposition (5 to 8 nm) for electrons to move through the tunneling mechanism in the system. Hence, the rheological percolation threshold is often lower than its electrical counterpart, except in limited cases, such as when the polymer chains themselves are partially conductive and assist in the transfer of electrical charge to GNPs [44]. Figure 12 nicely illustrated the two rheological and electrical percolation occurrences [43]. Kashi *et al*. [42] also stated in their study on PLA/GNP nanocomposites that temperature can affect the microstructure of nanocomposites and thus its viscoelastic properties. They showed that the rheological percolation threshold could be changed by altering the temperature conditions of the samples so that by increasing the temperature from 180 to 220 °C, the percolation range decreased from 9 to 6 wt% of GNPs. This rheological percolation threshold can also be within the range of the electrical percolation threshold.

3.7. Mechanical properties

There are several factors associated with the effectiveness of a tough elastomeric polymer, such as interfacial adhesion between blend components, type and concentration of elastomer, blending method, process conditions, and the shape and size of elastomeric particles. It is generally accepted that elastomeric particle size and interfacial adhesion between

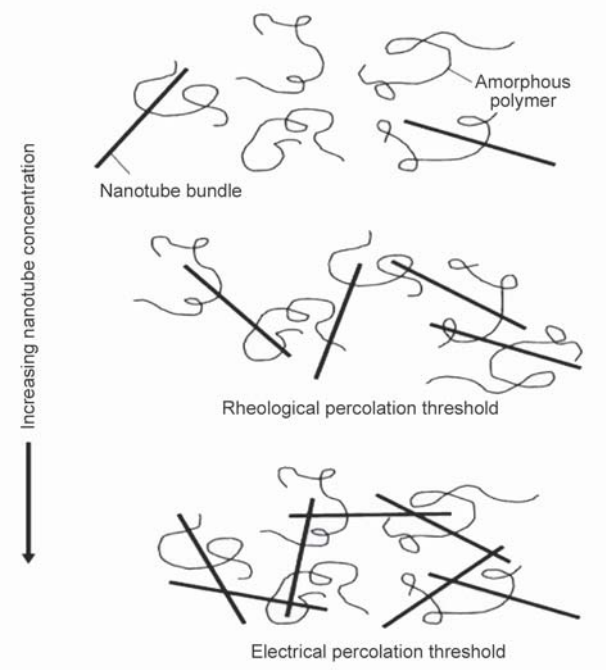

Figure 12. Rheological and electrical percolations scheme [41].

blend components have a vital role in determining the mechanical performance of a polymer blend. For example, larger particle size and poor adhesion lead to poor mechanical properties of the blend [35].

To evaluate the mechanical properties of blend PLA/POE/GNPs, the tensile test was performed on the samples. The tensile strength and elongation at the breakpoint of pure PLA and POE as well as the blend of these polymers without nanoplates and containing different amounts of GNPs were studied. The stress-strain curves of samples are shown in Figure 13 and the resulted values are reported in Table 4. The results revealed that PLA shows a completely brittle behavior with high tensile strength, and with the addition of POE, the tensile strength of the PLA/POE blend became less than the neat PLA. This is due to the elastomeric nature of POE and its low strength [45].

Table 4. Tensile strength and elongation to break of PLA/POE and PLA/POE/GNPs blends.

Sample	Tensile strength [MPa]	Elongation at break [%]
Pure POE	11.82±0.55	1609.87±89.36
Pure PLA	57.48±1.70	2.08±0.01
PLA60/POE40	16.59±0.11	5.20±0.01
PLA60/POE40/GNP0.2	18.75±0.77	4.83±0.23
PLA60/POE40/GNP0.5	20.92±0.04	4.59±0.91
PLA60/POE40/GNP1	24.37±0.55	4.54±0.98
PLA60/POE40/GNP1.5	25.32±0.76	4.42±0.35

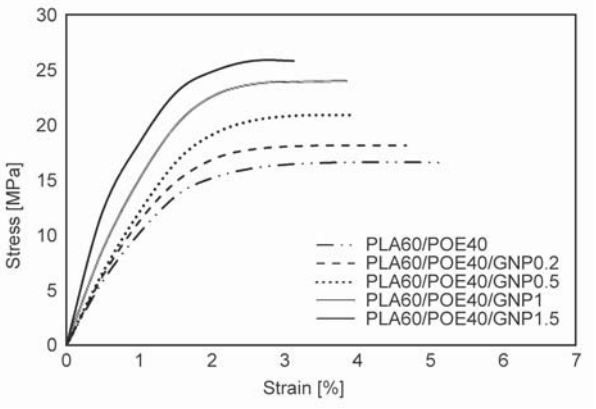

Figure 13. The effect of GNP on stress-strain curves of PLA60/POE 40 blend.

In contrast, the strain to breakpoint was increased from about 2% for PLA to about 2.5% for PLA/POE blend, indicating the effect of POE toughness on PLA. As the results showed, the tensile strength of the PLA/POE/GNPs blend increased linearly with the raising in GNPs quantities, which is attributed to the high strength of these mineral nanoplates. Reduction in elongation at break values was also observed for samples containing nanoplates. The improvement in tensile strength is due to the reinforcing effect and the relatively good dispersion of GNPs, which effectively transfer the stress from the polymer chains to the filler.

3.8. Comparison with previous works

A table-form comparison of the current study and the previous papers to specify the differences between them and to determine the novelty of this work is depicted in Table 5. As illustrated, in addition to the preparation of a three-component blend of POE/PLA/GNPs, Contact Angle (I), Surface tension (II), Morphological study (III), Electrical conductivity (IV), Rheological measurement (V), Mechanical properties (VI), and Percolation threshold (VII) are discussed in our study, which in other relevant works with different blend system and nanomaterials all of the noted properties were not discussed together.

4. Conclusions

A double percolation structure is an approach to decrease the amount of expensive nanographene filler in polymer blends. Blends of POE with biobased PLA led to the development of a semi-biodegradable material with acceptable toughness and flexibility. By localization of graphene in the POE phase in co-continuous POE/PLA blend, electrical percolation

Table 5. Comparison of current study with some published articles.

Authors	Blend phases	Nanomaterial	Preparation method	Contact angle (I), Surface tension (II), Morphological study (III), Electrical conductivity (IV), Rheological measurement (V), Mechanical properties (VI), Percolation threshold (VII)
Current study	PLA/POE	GNP	Melt mixing	I, II, III, IV, V, VI, VII
Bose *et al.* [36]	PA6/ABS	MWCNT	Melt mixing	III ,IV, V, VII
Xu *et al.* [46]	PLA/PCL	MWCNT	Melt compounding	III, IV, V
Mir *et al.* [44]	PMMA/POE	MWCNT	Solution casting	V, IV
Navas *et al.* [32]	PP/PS	MWCNT	Melt mixing	II, III, IV
Wang *et al.* [25]	PVDF/PLLA	Nanosilica (SiO_2)	Melt mixing	III, V, VII
Zhao *et al.* [26]	PVDF/PLLA	CNT with epoxy and PMMA-tails	Melt mixing	III, IV, VI, VII

threshold was achieved at 0.5 wt%, and electrical conductivity was increased by increasing graphene content. On the other hand, rheological properties were improved by adding graphene, and the rheological percolation threshold was started at 0.2 wt%. Mechanical properties, including tensile strength and elongation at break, were balanced by adding the POE and GNPs. It was found that diluting the prepared POE/graphene masterbatch is an efficient way to achieve better dispersion of graphene in the final blend.

References

[1] Sin L. T., Rahmat A. R., Rahman W. A. W. A.: Polylactic acid: PLA biopolymer technology and applications. Elsevier Amsterdam (2013).

[2] Doganay D., Coskun S., Kaynak C., Unalan H. E.: Electrical, mechanical and thermal properties of aligned silver nanowire/polylactide nanocomposite films. Composites Part B: Engineering, **99**, 288–296 (2016). https://doi.org/10.1016/j.compositesb.2016.06.044

[3] Jamshidian M., Tehrany E. A., Imran M., Jacquot M., Desobry S.: Poly-lactic acid: Production, applications, nanocomposites, and release studies. Comprehensive Reviews in Food Science and Food Safety, **9**, 552–571 (2010). https://doi.org/10.1111/j.1541-4337.2010.00126.x

[4] Di Y., Iannace S., Di Maio E., Nicolais L.: Reactively modified poly(lactic acid): Properties and foam processing. Macromolecular Materials and Engineering, **290**, 1083–1090 (2005). https://doi.org/10.1002/mame.200500115

[5] Utracki L. A.: Commercial polymer blends. Chapman and Hall, London (1998).

[6] Kresge E. N.: Polyolefin thermoplastic elastomer blends. Rubber Chemistry and Technology, **64**, 469–480 (1991). https://doi.org/10.5254/1.3538564

[7] Willemse R., de Boer A. P., van Dam J., Gotsis A.: *Co*-continuous morphologies in polymer blends: The influence of the interfacial tension. Polymer, **40**, 827–834 (1999). https://doi.org/10.1016/S0032-3861(98)00307-3

[8] Lyngaae-Jørgensen J., Rasmussen K. L., Chtcherbakova E. A., Utracki L. A.: Flow induced deformation of dual-phase continuity in polymer blends and alloys. Part I. Polymer Engineering and Science, **39**, 1060–1071 (1999). https://doi.org/10.1002/pen.11494

[9] Reddy K. R., Jeong H. M., Lee Y., Raghu A. V.: Synthesis of MWCNTs-core/thiophene polymer-sheath composite nanocables by a cationic surfactant-assisted chemical oxidative polymerization and their structural properties. Journal of Polymer Science Part A: Polymer Chemistry, **48**, 1477–1484 (2010). https://doi.org/10.1002/pola.23883

[10] Han S. J., Lee H-I., Jeong H. M., Kim B. K., Raghu A. V., Reddy K. R.: Graphene modified lipophilically by stearic acid and its composite with low density polyethylene. Journal of Macromolecular Science Part B, **53**, 1193–1204 (2014). https://doi.org/10.1080/00222348.2013.879804

[11] Kim H., Abdala A. A., Macosko C. W.: Graphene/polymer nanocomposites. Macromolecules, **43**, 6515–6530 (2010). https://doi.org/10.1021/ma100572e

[12] Gubbels F., Jerome R., Vanlathem E., Deltour R., Blacher S., Brouers F.: Kinetic and thermodynamic control of the selective localization of carbon black at the interface of immiscible polymer blends. Chemistry of Materials, **10**, 1227–1235 (1998). https://doi.org/10.1021/cm970594d

[13] Gu J., Zhang Q., Dang J., Yin C., Chen S.: Preparation and properties of polystyrene/SiCw/SiCp thermal conductivity composites. Journal of Applied Polymer Science, **124**, 132–137 (2012). https://doi.org/10.1002/app.35089

[14] Gu J., Lv Z., Wu Y., Zhao R., Tian L., Zhang Q.: Enhanced thermal conductivity of SiCp/PS composites by electrospinning–hot press technique. Composites Part A: Applied Science and Manufacturing, **79**, 8–13 (2015). https://doi.org/10.1016/j.compositesa.2015.09.005

[15] Zhao X., Zhao J., Cao J-P., Wang X., Chen M., Dang Z-M.: Tuning the dielectric properties of polystyrene/poly(vinylidene fluoride) blends by selectively localizing carbon black nanoparticles. The Journal of Physical Chemistry B, **117**, 2505–2515 (2013). https://doi.org/10.1021/jp310021r

[16] Pötschke P., Bhattacharyya A. R., Janke A.: Morphology and electrical resistivity of melt mixed blends of polyethylene and carbon nanotube filled polycarbonate. Polymer, **44**, 8061–8069 (2003). https://doi.org/10.1016/j.polymer.2003.10.003

[17] Du X., Skachko I., Barker A., Andrei E. Y.: Approaching ballistic transport in suspended graphene. Nature Nanotechnology, **3**, 491–495 (2008). https://doi.org/10.1038/nnano.2008.199

[18] Balandin A. A., Ghosh S., Bao W., Calizo I., Teweldebrhan D., Miao F., Lau C. N.: Superior thermal conductivity of single-layer graphene. Nano Letters, **8**, 902–907 (2008). https://doi.org/10.1021/nl0731872

[19] Lee C., Wei X., Kysar J. W., Hone J.: Measurement of the elastic properties and intrinsic strength of monolayer graphene. Science, **321**, 385–388 (2008). https://doi.org/10.1126/science.1157996

[20] Ho C-H., Wang C-H., Lin C-I., Lee Y-D.: Synthesis and characterization of TPO–PLA copolymer and its behavior as compatibilizer for PLA/TPO blends. Polymer, **49**, 3902–3910 (2008). https://doi.org/10.1016/j.polymer.2008.06.054

[21] Huang Y., Ellingford C., Bowen C., McNally T., Wu D., Wan C.: Tailoring the electrical and thermal conductivity of multi-component and multi-phase polymer composites. International Materials Reviews, **65**, 129–163 (2020). https://doi.org/10.1080/09506608.2019.1582180

[22] Marischal L., Cayla A., Lemort G., Campagne C., Devaux É.: Selection of immiscible polymer blends filled with carbon nanotubes for heating applications. Polymers, **11**, 1827/1–1827/16 (2019). https://doi.org/10.3390/polym11111827

[23] Hadaeghnia M., Ahmadi S., Ghasemi I., Wood-Adams P. M.: Manipulating the morphology of PA6/POE blends using graphene to achieve balanced electrical and mechanical properties. Composites Science and Technology, **200**, 108412/1–108412/10 (2020). https://doi.org/10.1016/j.compscitech.2020.108412

[24] Luo Y., Xiong S-Y., Zhang F., He X-X., Lu X., Peng R-T.: Preparation of conductive polylactic acid/high density polyethylene/carbon black composites with low percolation threshold by locating the carbon black at the interface of *co*-continuous blends. Journal of Applied Polymer Science, **138**, 50291/1–50291/11 (2020). https://doi.org/10.1002/app.50291

[25] Wang H., Yang X., Fu Z., Zhao X., Li Y., Li J.: Rheology of nanosilica-compatibilized immiscible polymer blends: Formation of a 'heterogeneous network' facilitated by interfacially anchored hybrid nanosilica. Macromolecules, **50**, 9494–9506 (2017). https://doi.org/10.1021/acs.macromol.7b02143

[26] Zhao X., Wang H., Fu Z., Li Y.: Enhanced interfacial adhesion by reactive carbon nanotubes: New route to high-performance immiscible polymer blend nanocomposites with simultaneously enhanced toughness, tensile strength, and electrical conductivity. ACS Applied Materials and Interfaces, **10**, 8411–8416 (2018). https://doi.org/10.1021/acsami.8b01704

[27] Paul D. R., Barlow J. W.: Polymer blends. Journal of Macromolecular Science Part C, **18**, 109–168 (1980). https://doi.org/10.1080/00222358008080917

[28] Miles I. S., Zurek A.: Preparation, structure, and properties of two-phase *co*-continuous polymer blends. Polymer Engineering and Science, **28**, 796–805 (1988). https://doi.org/10.1002/pen.760281205

[29] Xu D., Pop-Iliev R., Park C. B., Fenton R. G.: Fundamental study of CBA-blown bubble growth and collapse under atmospheric pressure. Journal of Cellular Plastics, **41**, 519–538 (2005). https://doi.org/10.1177/0021955X05059031

[30] De Rosa I. M., Sarasini F., Sarto M. S., Tamburrano A.: EMC impact of advanced carbon fiber/carbon nanotube reinforced composites for next-generation aerospace applications. IEEE Transactions on Electromagnetic Compatibility, **50**, 556–563 (2008). https://doi.org/10.1109/TEMC.2008.926818

[31] Ameli A., Jung P. U., Park C. B.: Electrical properties and electromagnetic interference shielding effectiveness of polypropylene/carbon fiber composite foams. Carbon, **60**, 379–391 (2013). https://doi.org/10.1016/j.carbon.2013.04.050

[32] Otero-Navas I., Arjmand M., Sundararaj U.: Carbon nanotube induced double percolation in polymer blends: Morphology, rheology and broadband dielectric properties. Polymer, **114**, 122–134 (2017). https://doi.org/10.1016/j.polymer.2017.02.082

[33] Singh A., Naskar A. K., Barden J., Drews M. J., Smith D. W.: Terpolymers from lactide and bisphenol a derivatives: Scale-up, properties, and blends. Journal of Applied Polymer Science, **122**, 2520–2528 (2011). https://doi.org/10.1002/app.33789

[34] Biresaw G., Carriere C. J.: Interfacial tension of poly (lactic acid)/polystyrene blends. Journal of Polymer Science Part B: Polymer Physics, **40**, 2248–2258 (2002). https://doi.org/10.1002/polb.10290

[35] Juntuek P., Ruksakulpiwat C., Chumsamrong P., Ruksakulpiwat Y.: Effect of glycidyl methacrylate-grafted natural rubber on physical properties of polylactic acid and natural rubber blends. Journal of Applied Polymer Science, **125**, 745–754 (2012). https://doi.org/10.1002/app.36263

[36] Bose S., Bhattacharyya A. R., Bondre A. P., Kulkarni A. R., Pötschke P.: Rheology, electrical conductivity, and the phase behavior of cocontinuous PA6/ABS blends with MWNT: Correlating the aspect ratio of MWNT with the percolation threshold. Journal of Polymer Science Part B: Polymer Physics, **46**, 1619–1631 (2008). https://doi.org/10.1002/polb.21501

[37] Min C., Shen X., Shi Z., Chen L., Xu Z.: The electrical properties and conducting mechanisms of carbon nanotube/polymer nanocomposites: A review. Polymer-Plastics Technology and Engineering, **49**, 1172–1181 (2010). https://doi.org/10.1080/03602559.2010.496405

[38] Zhang Q., Rastogi S., Chen D., Lippits D., Lemstra P. J.: Low percolation threshold in single-walled carbon nanotube/high density polyethylene composites prepared by melt processing technique. Carbon, **44**, 778–785 (2006). https://doi.org/10.1016/j.carbon.2005.09.039

[39] Wang M-J.: Effect of polymer-filler and filler-filler interactions on dynamic properties of filled vulcanizates. Rubber Chemistry and Technology, **71**, 520–589 (1998). https://doi.org/10.5254/1.3538492

[40] Friedrich C., Braun H.: Generalized cole-cole behavior and its rheological relevance. Rheologica Acta, **31**, 309–322 (1992). https://doi.org/10.1007/BF00418328

[41] Cole K. S., Cole R. H.: Dispersion and absorption in dielectrics I. Alternating current characteristics. The Journal of Chemical Physics, **9**, 341–351 (1941). https://doi.org/10.1063/1.1750906

[42] Kashi S., Gupta R. K., Baum T., Kao N., Bhattacharya S. N.: Phase transition and anomalous rheological behaviour of polylactide/graphene nanocomposites. Composites Part B: Engineering, **135**, 25–34 (2018). https://doi.org/10.1016/j.compositesb.2017.10.002

[43] Du F., Scogna R. C., Zhou W., Brand S., Fischer J. E., Winey K. I.: Nanotube networks in polymer nanocomposites: Rheology and electrical conductivity. Macromolecules, **37**, 9048–9055 (2004). https://doi.org/10.1021/ma049164g

[44] Mir S. M., Jafari S. H., Khonakdar H. A., Krause B., Pötschke P., Taheri Qazvini N.: A promising approach to low electrical percolation threshold in PMMA nanocomposites by using MWCNT-PEO predispersions. Materials and Design, **111**, 253–262 (2016). https://doi.org/10.1016/j.matdes.2016.08.073

[45] Pai F-C., Chu H-H., Lai S-M.: Reactive compatibilization of poly(lactic acid)/polyethylene octene copolymer blends with ethylene-glycidyl methacrylate copolymer. Journal of Polymer Engineering, **31**, 463–471 (2011). https://doi.org/10.1515/polyeng.2011.091

[46] Xu Z., Zhang Y., Wang Z., Sun N., Li H.: Enhancement of electrical conductivity by changing phase morphology for composites consisting of polylactide and poly (ε-caprolactone) filled with acid-oxidized multiwalled carbon nanotubes. ACS Applied Materials and Interfaces, **3**, 4858–4864 (2011). https://doi.org/10.1021/am201355j